

# Studying quantum spin systems through entanglement estimators

Tommaso Roscilde,<sup>1</sup> Paola Verrucchi,<sup>2</sup> Andrea Fubini,<sup>2</sup> Stephan Haas,<sup>1</sup> and Valerio Tognetti<sup>2,3</sup>

<sup>1</sup>*Department of Physics and Astronomy, University of Southern California, Los Angeles, CA 90089-0484*

<sup>2</sup>*Dipartimento di Fisica dell'Università di Firenze and Istituto Nazionale di Fisica della Materia, UdR Firenze, Via G. Sansone 1, I-50019 Sesto Fiorentino (FI), Italy*

<sup>3</sup>*Istituto Nazionale di Fisica Nucleare, Sezione di Firenze,*

*Via G. Sansone 1, I-50019 Sesto Fiorentino (FI), Italy*

(Dated: May 15, 2019)

We study the field dependence of the entanglement of formation in anisotropic  $S = 1/2$  antiferromagnetic chains displaying a  $T = 0$  field-driven quantum phase transition. The analysis is carried out via Quantum Monte Carlo simulations. At zero temperature the entanglement estimators show abrupt changes in the vicinity of the quantum phase transition, vanishing below the critical field, in correspondence with an exactly factorized state. By comparison with the exactly solvable case of a spin dimer, we notice that the above features are due to a genuine many-body effect, which is likely to persist in higher dimensions. Moreover, we single out a novel way of detecting the quantum phase transition of the system, based only on entanglement estimators. Entanglement properties provide therefore new insight in the ground state properties of quantum spin systems.

PACS numbers: 03.67.Mn, 75.10.Jm, 73.43.Nq, 05.30.-d

The occurrence of collective behavior in many-body quantum systems is associated with the development of classical correlations, as well as of correlations which cannot be accounted for in terms of classical physics, namely entanglement. Entanglement represents in essence the impossibility of giving a *local* description of a many-body quantum state. In particular entanglement is expected to play an essential role at quantum phase transitions, where quantum effects manifest themselves at all length scales. The behavior of entanglement at quantum phase transitions is a very recent topic, so far investigated in a few exactly solvable cases [1, 2, 3, 4]. Moreover, entanglement overwhelmingly comes into play in quantum computation and communication theory, being the main physical *resource* needed for their specific tasks [5]. In this respect, the perspective of manipulating entanglement by tunable quantum many-body effects appears very intriguing.

Spin-1/2 chains play a leading role in the actual scene since they naturally represent strings of quantum bits, and for the store of knowledge supplied by decades of theoretical, numerical and experimental research on one-dimensional(1D) magnetic systems.

In this Letter we consider a class of anisotropic spin chains displaying highly non-trivial behavior of entanglement properties upon changing an applied field. The hamiltonian has the form of an *XYZ model* in a field:

$$\hat{\mathcal{H}} = -J \sum_i \left[ \hat{S}_i^x \hat{S}_{i+1}^x + \Delta_y \hat{S}_i^y \hat{S}_{i+1}^y - \Delta_z \hat{S}_i^z \hat{S}_{i+1}^z + h \hat{S}_i^z \right] \quad (1)$$

where  $J > 0$  is the exchange coupling,  $i$  runs over the sites of the chain, and  $h \equiv g\mu_B H/J$  is the reduced magnetic field. The parameters  $\Delta_y, \Delta_z > 0$  control the anisotropy of the system. In particular, for  $\Delta_z = 0$  Eq. (1) reduces to the exactly solvable XY model in a transverse field [6]. For  $\Delta_z \neq 0$  the model does not in general admit

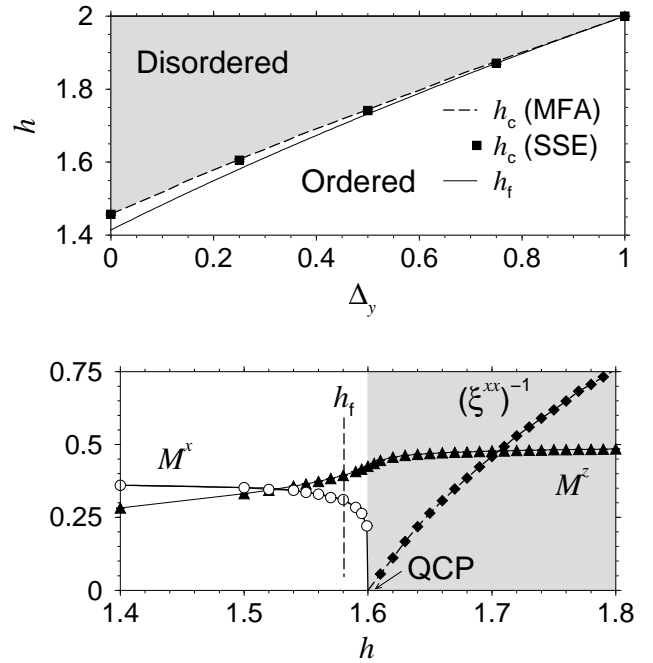


FIG. 1: Upper panel: ground state phase diagram of the XYX model in a field. Mean-field (MFA) results are taken from Ref. 10, the factorizing field  $h_f$  from Ref. 7. Lower panel: quantum critical behavior of  $x$ - and  $z$ -magnetizations and correlation length for the model with  $\Delta_y = 0.25$ ,  $L = 100$ ,  $\beta = 200$ . The factorizing field is indicated by a dashed line.

an exact solution [7], and it has been recently studied within approximate analytical and numerical approaches [8, 9, 10]. Interestingly, the general model with finite  $\Delta_z$  is experimentally realized by the  $S = 1/2$  quantum spin chain  $\text{Cs}_2\text{CoCl}_4$  [11], with strong planar XZ anisotropy,  $\Delta_y \approx 0.25$ ,  $\Delta_z \approx 1$ , and  $J \approx 0.23$  meV.

In our study, we concentrate on the case  $0 \leq \Delta_y \leq$

$\Delta_z = 1$ , defining the *XYX model* in a field. The more general case of the *XYZ* model in a magnetic field with  $\Delta_z < 1$  should exhibit the same qualitative behavior, as it shares the same symmetries with the *XYX* model in a field, and therefore it belongs to the same universality class. The analysis is carried out via Stochastic Series Expansion (SSE) Quantum Monte Carlo simulations, based on a modified directed-loop algorithm [12, 13], for chains of various length, from  $L = 40$  to  $L = 120$ . Ground state properties have been determined by considering inverse temperatures  $\beta = 2L$ , in order to capture the  $T = 0$  behaviour.

The ground-state phase diagram of the *XYX* model in the  $\Delta_y - h$  plane is shown in Fig. 1. The model displays a field-driven quantum phase transition at a critical field  $h_c(\Delta)$ , which separates the Néel-ordered phase ( $h \leq h_c$ ) from a partially-polarized disordered phase ( $h > h_c$ ). When  $h \leq h_c$  the field induces long-range magnetic order along the  $x$ -axis, giving rise to a finite magnetization estimated through the asymptotic value of the spin-spin correlator as  $M^x = |\langle \hat{S}_i^x \hat{S}_{i+L/2}^x \rangle|^{1/2}$ , where  $\langle \cdot \rangle$  denotes the ground-state expectation value. This magnetization vanishes at the critical field  $h_c$ , where magnetic correlations along  $x$  become short-ranged, while quantum fluctuations prevent the spins from being fully polarized along the field [7, 8, 10].

The transition line  $h_c(\Delta_y)$  has been determined by a detailed scaling analysis of the correlation length  $\xi^{xx}$ , whose linear scaling  $\xi^{xx} \sim L$  marks the quantum critical point. Our results are in very good agreement with predictions from mean-field approximation[8]. The predicted universality class, namely that of the 1D transverse Ising model [8], is well verified by the critical scaling of the structure factor  $S^{xx}(q = 0) \sim L^{\gamma/\nu-z}$  with  $\gamma/\nu = 7/4$  and  $z = 1$ .

Besides its quantum critical behavior, a striking feature of the model of Eq. (1) is the occurrence of an exactly factorized ground state for a field  $h_f(\Delta)$  lower than the critical field  $h_c$ , as predicted in Ref. [7]. In the case of the *XYX* model, this *factorizing field* is [7]  $h_f = \sqrt{2(1 + \Delta_y)}$ . At  $h = h_f$  the ground state of the model takes a product form  $|\Psi\rangle = \bigotimes_{i=1}^N |\psi_i\rangle$ , where the single-spin states  $|\psi_i\rangle$  are eigenstates of  $(\mathbf{n}_{1(2)} \cdot \hat{\mathbf{S}})$  with  $\mathbf{n}_{1(2)}$  being the local spin orientation on sublattice 1 (2). Taking  $\mathbf{n} = (\cos \phi \sin \theta, \sin \phi \sin \theta, \cos \theta)$ , one obtains [7]  $\phi_1 = 0$ ,  $\phi_2 = \pi$ ,  $\theta_1 = \theta_2 = \cos^{-1} \sqrt{(1 + \Delta_y)/2}$ . The factorized state of the anisotropic model continuously connects with the fully polarized state of the isotropic model in a field for  $\Delta_y = 1$  and  $h = 2$ .

Despite its exceptional character, the occurrence of a factorized state is not marked by any particular anomaly in the experimentally measurable thermodynamic quantities shown in the lower panel of Fig. 1. However, we will now see how the entanglement estimators are able to pin down the occurrence of a factorized state with high

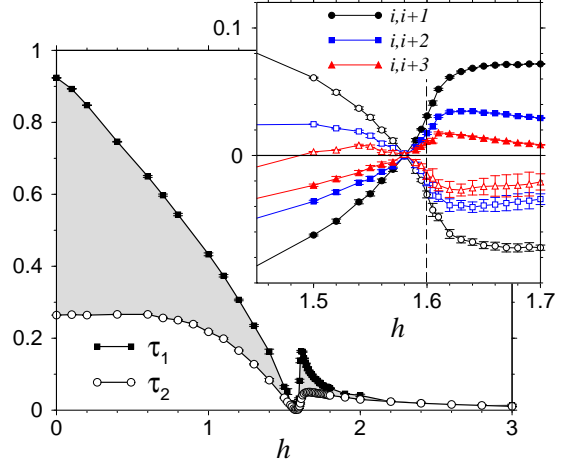


FIG. 2: One-tangle  $\tau_1$  and sum of squared concurrences  $\tau_2$  as a function of the applied field for the  $S = 1/2$  XYX model with  $\Delta_y = 0.25$ ,  $L = 100$  and  $\beta = 200$ . Inset: contributions to the concurrence between  $j$ -th neighbors; full symbols stand for  $C_{i,i+j}^{(1)}$ , open symbols for  $C_{i,i+j}^{(2)}$ . The dashed line marks the critical field  $h_c$ .

accuracy.

To estimate the *entanglement of formation* [14] in the quantum spin chain of Eq. (1) we make use of the *one-tangle* and of the *concurrence*. The one-tangle [15, 16] quantifies the  $T = 0$  entanglement of a single spin with the rest of the system. It is defined as  $\tau_1 = 4 \det \rho^{(1)}$ , where  $\rho^{(1)} = (I + \sum_\alpha M^\alpha \sigma^\alpha)/2$  is the one-site reduced density matrix,  $M^\alpha = \langle \hat{S}^\alpha \rangle$ ,  $\sigma^\alpha$  are the Pauli matrices, and  $\alpha = x, y, z$ . In terms of the spin expectation values  $M^\alpha$ ,  $\tau_1$  takes the simple form:

$$\tau_1 = 1 - 4 \sum_\alpha (M^\alpha)^2. \quad (2)$$

The concurrence [17] quantifies instead the pairwise entanglement between two spins at sites  $i, j$  both at zero and finite temperature. For the model of interest, in absence of spontaneous symmetry breaking ( $M^x = 0$ ) the concurrence takes the form [16]

$$C_{ij} = 2 \max\{0, C_{ij}^{(1)}, C_{ij}^{(2)}\}, \quad (3)$$

where

$$C_{ij}^{(1)} = g_{ij}^{zz} - \frac{1}{4} + |g_{ij}^{xx} - g_{ij}^{yy}|, \quad (4)$$

$$C_{ij}^{(2)} = |g_{ij}^{xx} + g_{ij}^{yy}| - \sqrt{\left(\frac{1}{4} + g_{ij}^{zz}\right)^2 - (M^z)^2}, \quad (5)$$

with  $g_{ij}^{\alpha\alpha} = \langle \hat{S}_i^\alpha \hat{S}_j^\alpha \rangle$ .

The  $T = 0$  QMC results for the model Eq. (1) with  $\Delta_y = 0.25$  are shown in Fig. 2, where we plot  $\tau_1$ , the sum of squared concurrences

$$\tau_2 = \sum_{j \neq i} C_{ij}^2, \quad (6)$$

and, in the inset,  $C_{i,i+n}$  for  $n = 1, 2, 3$ . The following discussion, although directly referred to the results for  $\Delta_y = 0.25$ , is actually quite general and applies to all the other studied values of  $\Delta_y$ .

Unlike the standard magnetic observables plotted in Fig. 1, the entanglement estimators display a marked anomaly at the factorizing field, where they clearly vanish as expected for a factorized state. When the field is increased above  $h_f$ , the ground-state entanglement has a very steep recovery, accompanied by the quantum phase transition at  $h_c > h_f$ . The system realizes therefore an interesting *entanglement switch* effect controlled by the magnetic field. We will discuss later how this effect is genuinely associated with the many-body behavior of the system.

As for the concurrence terms Eqs. (4),(5), we notice that they generally stay short-ranged, and usually never extend farther than the third neighbor. The longest range of  $C_{ij}$  is indeed observed around the factorizing field  $h_f$  and around the quantum critical point  $h_c$ . Moreover, the factorizing field divides two field regions with different expressions for the concurrence:

$$C_{ij}^{(1)} < 0 < C_{ij}^{(2)} \quad \text{for } h < h_f, \quad (7)$$

$$C_{ij}^{(2)} < 0 < C_{ij}^{(1)} \quad \text{for } h > h_f, \quad (8)$$

whereas  $C_{ij}^{(1)} = C_{ij}^{(2)} = 0$  at  $h = h_f$ .

In presence of spontaneous symmetry breaking occurring for  $h < h_c$ , the expression of the concurrence is generally expected to change with respect to Eqs. (4),(5), as extensively discussed in Ref. 18. For the model under investigation, this happens when the condition [18]  $C_{ij}^{(2)} < C_{ij}^{(1)}$  is satisfied, i.e. for  $h > h_f$ . This means that our estimated concurrence is accurate even in the ordered phase above the factorizing field; in the region  $0 < h < h_f$  it represents instead a lower bound to the actual  $T = 0$  concurrence. Alternatively it can be regarded as the concurrence for infinitesimally small but finite temperature.

In Fig. 2 the sum of squared concurrences  $\tau_2$  is seen to be always smaller than or equal to the one-tangle  $\tau_1$ , in agreement with the Coffman-Kundu-Wootters conjecture [15]. This shows that entanglement is only partially stored in two-spin correlations, and it is present also at the level of three-spin entanglement, four-spin entanglement, etc. In particular, we interpret the *entanglement ratio*  $R = \tau_2/\tau_1$  as a measure of the fraction of the total entanglement stored in *pairwise* correlations. This ratio is plotted as a function of the field in Fig. 3. As the field increases, we observe the general trend of pairwise entanglement saturating the whole entanglement content of the system. But a striking anomaly occurs at the quantum critical field  $h_c$ , where  $R$  displays a very narrow dip. According to our interpretation, this result shows that the weight of pairwise entanglement decreases dramatically at the quantum critical point in favour of multi-spin

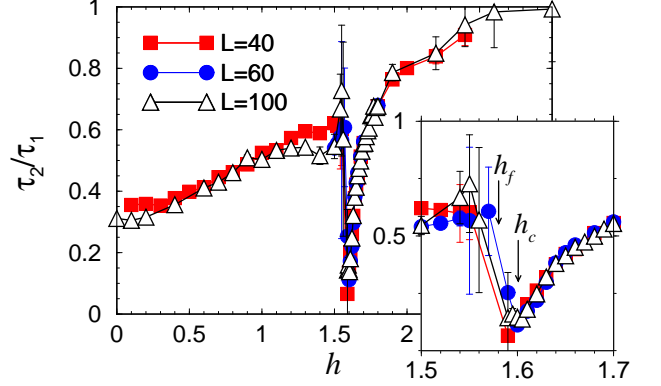


FIG. 3: Entanglement ratio  $\tau_2/\tau_1$  as a function of the field for  $\Delta_y = 0.25$  and  $\beta = 2L$ . Inset: zoom on the critical region.

entanglement. Unlike classical-like correlations, entanglement shows the special property of *monogamy* [15], namely full entanglement between two partners implies the absence of entanglement with the rest of the system. Therefore multi-spin entanglement appears as the only possible quantum counterpart to long-range spin-spin correlations occurring at a quantum phase transition. This also explains the somewhat puzzling result that the concurrence remains short-ranged at a quantum phase transition while the spin-spin correlators become long-ranged [1], and it evidences the serious limitations of concurrence as an estimate of entanglement at a quantum critical point. In turn, we propose the minimum of the entanglement ratio  $R$  as a novel estimator of the quantum critical point, fully based on entanglement quantifiers.

The use of the quantum Monte Carlo method enables us to naturally monitor the fate of entanglement when the temperature is raised above zero. In this regime the concurrence is the only well-defined estimator of entanglement, whereas the one-tangle has not yet received a finite-temperature generalization. Fig. 4 shows the nearest-neighbor concurrence as a function of temperature and field for the XYX model with  $\Delta_y = 0$ . The most prominent feature is the persistence of a vanishing point for the concurrence as the temperature is raised above zero. This feature is also observed for larger distances than nearest neighbors. This means that the factorizing effect of the field persists at finite temperature, resisting *thermal entanglement* [19], at least at the level of pairwise correlations. A simple explanation to this behavior is provided by the excitation spectrum on top of the factorized ground state. In fact, the field induces a gap to the first excited state, estimated to be around  $0.1J$  at  $h = h_f$  for  $\Delta_y = 0$  [8]. Therefore thermal mixing of the factorized ground state with excited entangled states is prevented by this gap up to temperatures comparable to the gap energy. Indeed, we do observe thermal entanglement occurring at  $h \approx h_f$  for  $T \gtrsim 0.1J$ , as clearly shown in Fig. 4. When  $T$  gets larger than the gap, the system

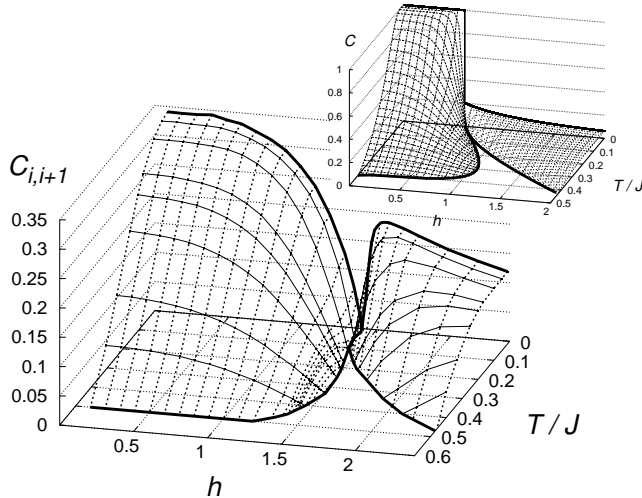


FIG. 4: Nearest neighbor concurrence  $C_{i,i+1}$  as a function of temperature and field for the XYX model with  $\Delta_y = 0$ ,  $L = 40$ . Inset: concurrence as a function of temperature and field for the XYX dimer with  $\Delta_y = 0$ . The thick solid lines trace the zeroes of the concurrence and its field dependence at  $T = 0$ .

begins to display a vanishing concurrence in a finite field interval, larger the higher the temperature, until this interval coincides with the whole field range at  $T \approx 0.5J$ .

To further understand the role of many-body effects on entanglement, we compare our results for the spin chain with the exactly solvable case of an XYX spin dimer in a magnetic field [20]. In this case the concurrence accounts for the whole entanglement of the system. The concurrence for the spin dimer system with  $\Delta_y = 0$  as a function of field and temperature is shown in the inset of Fig. 4. We observe that rigorously at  $T = 0$  the concurrence shows a step-like behavior at a field  $h = h_s$ , but it *never vanishes*, as the system does not admit a factorized ground state, no matter the value of the field. Nonetheless, as soon as the temperature is raised above zero, the concurrence vanishes at  $h \approx h_s$  under the effect of thermal fluctuations. We notice that, embedding a spin dimer inside a spin chain, even at  $T = 0$  the effect of the many-body environment on the dimer is to force the spins to fluctuate out of their isolated ground state, introducing in a sense an effective finite temperature for the dimers building the spin chain, and then leading to the factorization of the ground state for the whole spin chain.

In summary, making use of efficient quantum Monte Carlo techniques we have provided a comprehensive picture of the entanglement properties in a class of anisotropic spin chains of relevance to experimental compounds. We have shown that the occurrence of a classical factorized state in these systems is remarkably singled out by entanglement estimators, unlike the more conven-

tional magnetic observables. Moreover we find that the entanglement estimators are able to detect the quantum critical point, marked by a narrow dip in the pairwise-to-global entanglement ratio. Therefore we have shown that entanglement estimators provide a precious insight in the ground-state properties of lattice  $S = 1/2$  spin systems. Thanks to the versatility of quantum Monte Carlo, the same approach can be used for higher-dimensional systems. In this respect, investigations of the occurrence of factorized states in more than one dimension are currently in progress. Finally, the proximity of a quantum critical point to the factorized state of the system gives rise to an interesting field-driven entanglement-switch effect. This demonstrates that many-body effects driven by a macroscopic field are a powerful tool for the control of the microscopic entanglement in a multi-qubit system, and stand as a profitable resource for quantum computing devices.

Fruitful discussions with T. Brun, P. Delsing, and G. Vidal are gratefully acknowledged. We acknowledge support by DOE under grant DE-FG03-01ER45908 (T.R. and S.H.), by INFN, INFM, and MIUR-COFIN2002 (A.F., P.V., and V.T.).

---

- [1] A. Osterloh *et al.*, Nature (London) **416**, 608 (2002).
- [2] T.J. Osborne *et al.*, Phys. Rev. A **66**, 032110 (2002).
- [3] G. Vidal *et al.*, Phys. Rev. Lett. **90**, 227902 (2003).
- [4] F. Verstraete *et al.*, Phys. Rev. Lett. **92**, 027901 (2004).
- [5] M. A. Nielsen and I. L Chuang, *Quantum Computation and Quantum Information*, Cambridge Univ. Press, 2000.
- [6] E. Barouch *et al.*, Phys. Rev. A **2**, 1075 (1970); *ibid.* **3**, 786 (1971).
- [7] J. Kurmann *et al.*, Physica A, **112**, 235 (1982).
- [8] D. V. Dmitriev *et al.*, J. Exp. Th. Phys. **95**, 538 (2002).
- [9] F. Capraro and C. Gros, Eur. Phys. J B **29**, 35 (2002).
- [10] J.-S. Caux *et al.*, Phys. Rev. E **68**, 134431 (2003).
- [11] M. Kenzelmann *et al.*, Phys. Rev. B **65**, 144432 (2002).
- [12] O. F. Syljuåsen *et al.*, Phys. Rev. E **66**, 046701 (2002).
- [13] The original directed-loop algorithm was designed to treat models with a continuous rotational symmetry in the plane transverse to the field. We have therefore generalized it to our less symmetric model introducing further vertices not conserving the  $z$ -magnetization, associated with the operators  $S_i^+ S_{i+1}^+$  and  $S_i^- S_{i+1}^-$  appearing in our hamiltonian with quantization axis along  $z$ , and minimizing the bounce probability as in the original scheme of Ref. 12. Details of the algorithm will be presented elsewhere.
- [14] C. H. Bennett *et al.*, Phys. Rev. A **54**, 3824 (1996).
- [15] V. Coffman *et al.*, Phys. Rev. A, **61** 052306 (2000).
- [16] L. Amico *et al.*, Phys. Rev. A **69**, 022304 (2004).
- [17] W.K. Wootters, Phys. Rev. Lett. **80**, 2245 (1998).
- [18] O.F. Syljuåsen, Phys. Rev. A **68**, 060301 (2003).
- [19] M.C. Arnesen *et al.*, Phys. Rev. Lett. **87**, 017901 (2001).
- [20] L. Zhou *et al.*, Phys. Rev. A **68**, 024301 (2003).